ISET Journal of Earthquake Technology, Paper No. 437, Vol. 40, No. 2-4, June-December 2003, pp. 161-172

MOMENT SOLUTIONS OF ANTI-PLANE (SH) WAVE DIFFRACTION AROUND ARBITRARY-SHAPED RIGID FOUNDATIONS ON A WEDGE-SHAPE HALF SPACE

Nazaret Dermendjian* and Vincent W. Lee**

*Assistant Professor, Department of Civil Engineering and Applied Mechanics
California State University, Northridge, California 91330-8347, U.S.A.

**Professor, Civil and Environmental Engineering Department
University of Southern California, Los Angeles, California 90089-2531, U.S.A.

ABSTRACT

The dynamic response and wave propagation behavior resulting from anti-plane diffraction around an elastic wedge-shaped medium with an arbitrary-shaped cylindrical rigid foundation at its vertex has been studied. Numerical computation of the wave displacement field is carried out on and near the rigid foundation surfaces using the method of weighted-residuals, also known as the moment method. The wave displacement fields for the cases of elliptic, circular, rounded-rectangular and flat-elliptic rigid foundations are presented. As in previous works, the analysis demonstrates that the resulting surface displacement depends on many factors, including 1) the angle of the wedge-shaped half space, 2) the density (measure of rigidity) of the foundation, its geometry or shape at the vertex, 3) the frequencies of the incident waves, 4) the angle of incidence, and 5) the material properties of the media. The analysis provides results that help to explain geophysical observations regarding the amplification of seismic energy as a function of site conditions.

KEYWORDS: Waves, Weighted-Residues, Wedge, Arbitrary-Shaped, Foundations

INTRODUCTION

The research presented in this paper involves the study of plane SH-waves propagating through a wedge-shaped media. In particular, the geometry of the media ranges from a flat elastic half-space (where the wedge angle is 180°) through the sloping wedge-shaped half space with wedge angles ($\nu\pi$, $\frac{1}{2} \leq \nu \leq 1$) ranging between 180° and 90° from a half space ($\nu = 1$) to a quarter-space ($\nu = \frac{1}{2}$). Furthermore, an arbitrary-shaped and dynamically movable rigid foundation is present at the vertex of the wedge. Figure 1 illustrates the geometry of a sloping wedge-shape half space for the case of incident plane SH-waves.

Even though the treatment of the problem is somewhat mathematical, it is believed that the consideration of such a problem has practical ramifications, as many houses and other structures have been built on ridges and cliffs overlooking valleys and the ocean. The topography of these ridges can be reasonably characterized in two-dimensions as a wedge-shaped half space.

The problem of the two-dimensional scattering and diffraction of plane elastic SH (shear horizontal, anti-plane) waves by a surface cylindrical canyon or rigid foundation in an elastic half-space has been studied by many researchers in earthquake engineering and strong-motion seismology. Trifunac (1973) first solved such two-dimensional SH scattering and diffraction of plane SH waves by a semi-circular canyon and later by rigid foundation in a flat elastic half space (Luco et al., 1975). Wong and Trifunac (1974a, 1974b) solved the same problem for semi-elliptical canyons, rigid foundations and alluvial valleys. Cao and Lee (1989, 1990), Lee and Cao (1989) extended Trifunac's results (Trifunac, 1973) to cases involving shallow circular canyons, respectively, for incident SH, P and SV waves. Lee (1982, 1984, 1988, 1990) further studied diffraction problems for hemispherical canyons, valleys and parabolic canyons. The common feature of the above papers is that all of the canyons are either circular, elliptic or parabolic in shape. In other words, they are all of regular shapes. This allows all of the above analyses to give closed-form analytic series as solutions to the problems. Good references for elastic wave propagation problems are found in texts by Mow and Pao (1971), Achenbach (1973), and Graff (1991).

For canyons, valleys or rigid foundations with irregular shapes, field computations will have to be carried out by numerical approximations (Wong et al., 1977; Sanchez-Sesma and Rosenbleuth, 1979).

Some popular methods in the analyses of wave diffractions are the finite difference method (FDM), the finite element method (FEM), and the boundary element method (BEM).

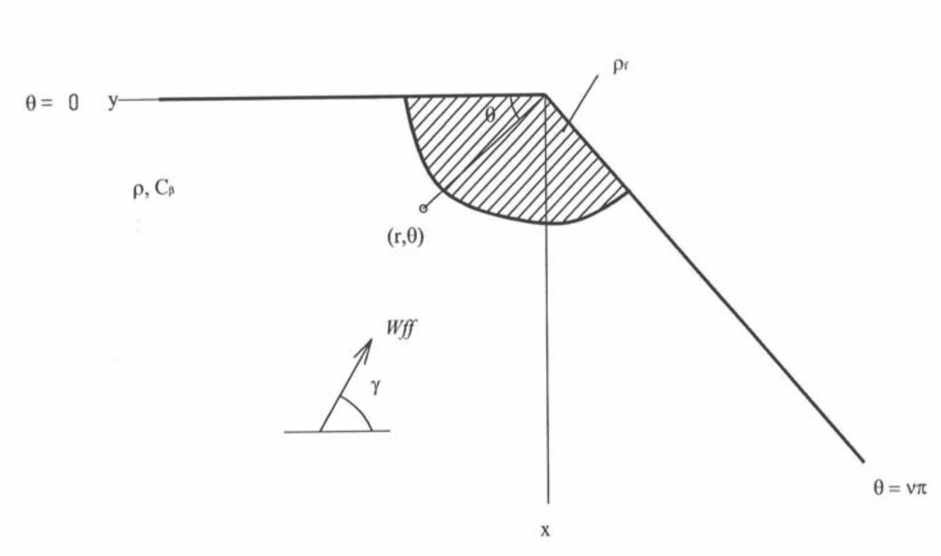

Fig. 1 Arbitrary-shaped rigid foundation - The model

As pointed out in Lee and Wu (1994a, 1994b), with FDM or FEM, material inhomogeneity and irregular geometry can be modeled easily. But in dealing with semi-infinite or infinite domains, which are usually associated with the problem of wave scattering and diffraction, some approximations have to be introduced. The most general method is to simply truncate the infinite or semi-infinite domains into finite ones. In this way, artificial boundaries will have to be created and they will prevent the true propagation of the waves, thus introducing errors. Another difficulty is that FDM and FEM may be easily overwhelmed by the large physical dimensions or the fine details of the requirement, so for seismic wave analysis in a semi-infinite domain, they would numerically become a large-sized problem. The BEM, on the other hand, does not have these disadvantages; it only needs to perform integration along the boundaries and model the infinite domain very well. Theoretically, it is very suitable for the problems with infinite or semi-infinite geometries. It, however, encounters difficulty in dealing with the Green's function singularities in the path of numerical integration.

With this difficulty in mind, Lee and Wu (1994a, 1994b) chose instead the so-called "weighted residual" or "moment" method to solve these diffraction problems involving arbitrary-shaped rigid foundations. This method is used abundantly both in the fields involving electromagnetic and acoustic waves. See Harrington (1967) for a full historical development and references of this method.

In the weighted residual method, used in this study, like the BEM, it only needs to be integrated along the original boundaries. Thus, the size of the equations is greatly reduced, when compared with that of the FDM and FEM, and it imposes no artificial boundaries at all. It also does not involve the Green's function, thus avoiding the difficulty of singularities that the other methods encounter. Compared with the method of using the simple full space Green's function (Chang, 1990), the results of the weighted residual method are much better for relatively deep rigid foundations. Besides all of these advantages, it is also simple to formulate. So the weighted residual, proposed here, is very suitable for wave scattering and diffraction problems. It is applied to arbitrary-shaped rigid foundations in this paper.

Lee and Sherif (1996) presented such a diffraction problem involving a circular canyon at the vertex of the wedge space. The solution is expressible in simple analytic closed form involving Hankel functions with the corresponding cosine terms. The analysis indicates that SH-waves travelling through a particular wedge geometry result in displacement fields that depend on the angle of incidence, the frequency of the incident wave, the geometry of the vertex and the material properties of the media.

General research in diffraction problems involving elastic wedge-shaped half spaces are very mathematical and is ongoing. A general literature survey of the current status of such research can be found in the lecture notes by Croisille and Lebeau (1999). Examples of more recent publications of elastic wedge problems are Pozharski (2000), and Marzeda et al. (2003).

SH WAVE PROPAGATION IN AN ELASTIC WEDGE

The two-dimensional model of the problem is shown in Figure 1. It represents the wedge-shaped space with angle $\nu\pi$, where $1/2 < \nu < 1$. An arbitrary-shaped rigid foundation is situated on the vertex of the wedge space. Both the rectangular (x,y) and cylindrical (r,θ) coordinate systems are defined on the model. The wedge-shaped space is assumed to be elastic, isotropic and homogeneous, with the material properties given by Lame constants λ and μ and by the mass density ρ, from which the shear wave speed, $C_\beta = (\mu/\rho)^{1/2}$, is derived.

For incident plane SH waves with incident angle γ with respect to the horizontal, the free-field equation is (Sanchez-Sesma, 1985; Lee and Sherif, 1996)

$$W^{ff} = \frac{2}{\nu}\sum_{n=0}^{\infty}\varepsilon_n e^{\frac{-in\pi}{2\nu}} J_{\frac{n}{\nu}}(kr)\cos(\frac{n\gamma}{\nu})\cos(\frac{n\theta}{\nu}) \tag{1}$$

where $\varepsilon_0 = 1$, and $\varepsilon_n = 2$ for $n > 0$. The presence of the arbitrary-shaped rigid foundation will result in the scattered waves which are given by the equation (Lee and Sherif, 1996):

$$W^s = \sum_{n=0}^{\infty} A_n H^{(1)}_{\frac{n}{\nu}}(kr)\cos(\frac{n\theta}{\nu}) \tag{2}$$

Both the free-field W^{ff} and scattered waves W^s satisfy the free-field boundary condition:

$$\tau_{z\theta} = \frac{\mu}{r}\frac{\partial}{\partial\theta}W^s = 0, \quad \text{at } \theta = 0,\ \nu\pi \tag{3}$$

At $r > a(\theta)$, and $\theta = 0$ and $\theta = \nu\pi$, the free-field stress boundary conditions are satisfied by W^{ff} and W^s. Let the displacement of rigid foundation be denoted by Δ. At C, the surface of the rigid foundation, the displacement continuity boundary condition for $r = a(\theta)$, $0 \le \theta \le \nu\pi$, is

$$\left(W^{ff} + W^s\right)\Big|_{r=a(\theta)} = \Delta \tag{4}$$

THE WEIGHTED RESIDUAL (MOMENT) METHOD

The weighted residual method, also known as the moment method, is used as a numerical method for the evaluation of the displacement field (Lee and Wu, 1994a, 1994b; Lee and Manoogian, 1995). Weight functions are selected along the surface of the rigid foundation C, such that $w_m = w_m(\theta)$ for $m = 0,1,2,3,\ldots$ and along C.

Using a weight function of $w_m(\theta) = \cos(m\theta/\nu)$, the above equation can be represented by

$$\int_0^{\nu\pi}\left(W^{ff} + W^s - \Delta\right)\Big|_{r=a(\theta)}\cos\left(\frac{m\theta}{\nu}\right)d\theta = 0 \tag{5}$$

The unknown coefficients are in the series of W^s, and thus Equation (5) may be rewritten as, for $m = 0, 1, 2, \ldots$

$$\int_0^{\nu\pi} W^s\Big|_{r=a(\theta)}\cos\left(\frac{m\theta}{\nu}\right)d\theta = \int_0^{\nu\pi}\left(\Delta - W^{ff}\right)\Big|_{r=a[\theta]}\cos\left(\frac{m\theta}{\nu}\right)d\theta \tag{6}$$

For $m = 0$, Equation (6) reduces to

$$\begin{aligned}&\int_0^{\nu\pi}\sum_{n=0}^{\infty} A_n H^{(1)}_{n/\nu}(ka(\theta))\cos\left(\frac{n\theta}{\nu}\right).d\theta \\ &= \int_0^{\nu\pi}\Delta.d\theta - \int_0^{\nu\pi}\sum_{n=0}^{\infty} a_n J_{n/\nu}(ka(\theta))\cos\left(\frac{n\theta}{\nu}\right).d\theta\end{aligned} \tag{7}$$

Equation (7) can be represented by

$$\sum_{n=0}^{\infty} C_{0n} A_n - \Delta \nu \pi = -\sum_{n=0}^{\infty} c_{0n} a_n \tag{8}$$

where the unknowns are A_n and Δ. The coefficients C_{0n} and c_{0n} are shown below.

$$\left.\begin{aligned} C_{0n} &= \int_0^{\nu\pi} H^{(1)}_{n/\nu}(ka(\theta))\cos\left(\frac{n\theta}{\nu}\right).d\theta \\ c_{0n} &= \int_0^{\nu\pi} J_{n/\nu}(ka(\theta))\cos\left(\frac{n\theta}{\nu}\right).d\theta \end{aligned}\right\} \tag{9}$$

Note that the term c_{0n} is the real part of C_{0n}, $c_{0n} = \text{Re}(C_{0n})$, for $n = 0, 1, 2, \ldots$.

For $m > 0$, the respective equations become

$$\begin{aligned} &\int_0^{\nu\pi} \sum_{n=0}^{\infty} A_n H^{(1)}_{n/\nu}(ka(\theta)).\cos\left(\frac{n\theta}{\nu}\right).\cos\left(\frac{m\theta}{\nu}\right).d\theta \\ &= -\int_0^{\nu\pi} \sum_{n=0}^{\infty} a_n J_{n/\nu}(ka(\theta)).\cos\left(\frac{n\theta}{\nu}\right).\cos\left(\frac{m\theta}{\nu}\right).d\theta \end{aligned} \tag{10}$$

from the fact that the Δ term drops out, because for $m > 0$,

$$\int_0^{\nu\pi} \Delta\cos\left(\frac{m\theta}{\nu}\right)d\theta = \Delta\int_0^{\nu\pi} \cos\left(\frac{m\theta}{\nu}\right)d\theta = 0 \tag{11}$$

Equation (10) can be represented by

$$\sum_{n=0}^{\infty} C_{mn} A_n = -\sum_{n=0}^{\infty} c_{mn} a_n \tag{12}$$

with the coefficients A_n, $n = 0, 1, 2, \ldots$ The coefficients C_{mn} and c_{mn} are shown below:

$$\left.\begin{aligned} C_{mn} &= \int_0^{\nu\pi} H^{(1)}_{n/\nu}(ka(\theta)).\cos\left(\frac{n\theta}{\nu}\right)\cos\left(\frac{m\theta}{\nu}\right).d\theta \\ c_{mn} &= \int_0^{\nu\pi} J_{n/\nu}(ka(\theta)).\cos\left(\frac{n\theta}{\nu}\right)\cos\left(\frac{m\theta}{\nu}\right).d\theta \end{aligned}\right\} \tag{13}$$

Again, c_{mn} is the real part of C_{mn}, i.e. $c_{mn} = \text{Re}(C_{mn})$.

THE KINETIC EQUATION

Unlike the case of a semi-circular canyon in an elastic wedge-shaped half space (Dermendjian and Lee, 2001), the above equations were enough to solve for the unknown A_ns, as there was no rigid displacement, Δ, term. Thus, the kinetic equation is utilized for the additional equation. The kinetic equation is

$$f_z^s = -\omega^2 M_f \Delta \tag{14}$$

where M_f is the mass of the foundation, the shaded area of Figure 1, and f_z^s is the force of the resultant waves $W = W^{ff} + W^s$ acting onto the surface of the foundation per unit z length. Also note that ω may be expressed in terms of the shear wave number k, the shear modulus μ, and the mass density ρ. The kinetic equation becomes

$$\omega^2 = k^2 c^2 = k^2 \frac{\mu}{\rho} \tag{15}$$

$$f_z^s = -k^2 \mu \frac{\rho_f}{\rho} A\Delta \tag{16}$$

where M_f is replaced by $\rho_f A$, A being the cross-section area of the foundation.

The force per unit length in the z direction, acting on the rigid foundation, the shaded portion of Figure 1, is evaluated in terms of the stresses acting on the rigid foundation, i.e.

$$f_z^s = \int_0^{\nu\pi} \tau_{nz}\Big|_{r=a(\theta)} \frac{a(\theta)}{\cos(\alpha(\theta))} d\theta \tag{17}$$

In Equation (17), $\alpha = \alpha(\theta)$ represents the angle between the radial and normal directions, and τ_{nz} is given by the equation below

$$\tau_{nz} = \mu \frac{\partial W}{\partial n} = \mu \left(\frac{\partial W}{\partial r} n_r + \frac{\partial W}{\partial \theta} n_\theta \right) \tag{18}$$

where $W = W^{ff} + W^s$ is the total displacement field, $n_r = \cos\alpha$ and $n_\theta = \sin\alpha$. Substituting Equation (16) into Equation (15) and combining with Equation (14), the following relationships are developed:

$$\sum_{n=0}^{\infty} D_n A_n + \left(\frac{\rho_f}{\rho} \right) k^2 A.\Delta = -\sum_{n=0}^{\infty} d_n a_n \tag{19}$$

with the unknowns of A_n and Δ. The coefficients D_n and d_n are given below:

$$\left.\begin{aligned} D_n &= \int_0^{\nu\pi} \left(H_{n/\nu}^{(1)'}(ka(\theta)) \cos\left(\frac{n\theta}{\nu} \right) a(\theta) - \frac{n}{\nu} H_{n/\nu}^{(1)}(ka(\theta)) \sin\left(\frac{n\theta}{\nu} \right) \tan(\alpha) \right) .d\theta \\ d_n &= \int_0^{\nu\pi} \left(J_{n/\nu}^{'}(ka(\theta)) \cos\left(\frac{n\theta}{\nu} \right) a(\theta) - \frac{n}{\nu} J_{n/\nu}(ka(\theta)) \sin\left(\frac{n\theta}{\nu} \right) \tan(\alpha) \right) .d\theta \end{aligned}\right\} \tag{20}$$

Again note that d_n is the real part of D_n, $d_n = \mathrm{Re}(D_n)$. Equations (8) and (19) yield the unknowns A_ns and Δ, and thus the displacement field is evaluated.

THE CASE OF A SEMI-CIRCULAR RIGID FOUNDATION

The case of the semi-circular foundation in an elastic wedge-shaped half space has an exact closed form solution for an incident plane SH wave (Dermendjian and Lee, 2001). The solution of the weighted-residual method can thus be compared with the exact solution. The free-field motion and the scattered waves are given earlier by Equations (1) and (3). The boundary condition, expressed earlier by Equation (4), is repeated here with the value of $r = a =$ constant, the radius of the rigid circular foundation.

$$(W^{ff} + W^s)\Big|_{r=a} = \Delta \tag{21}$$

Thus, the solution represented by Equations (7), (8) and (9) is repeated here with the change of $r = a$ rather than $r = a(\theta)$. The equations represented in Equations (9) are rewritten as

$$\left.\begin{aligned} C_{0n} &= H_{n/\nu}^{(1)}(ka) \int_0^{\nu\pi} \cos\left(\frac{n\theta}{\nu} \right) d\theta \\ c_{0n} &= J_{n/\nu}(ka) \int_0^{\nu\pi} \cos\left(\frac{n\theta}{\nu} \right) d\theta \end{aligned}\right\} \tag{22}$$

since the Hankel function of the first kind and the Bessel functions are independent of θ and thus can be taken out of the integral sign. The integrals in Equations (22) will vanish for all n not equal to 0, and have a value of $\nu\pi$ at $n = 0$. The equation represented by Equation (8) reduces to

$$H_0^{(1)}(ka).\nu\pi.A_0 - \Delta\nu\pi = -J_0(ka).\nu\pi.\frac{2}{\nu} \tag{23}$$

The other relationship relating A_0 and Δ is presented by utilizing Equations (14) through (18), and is given in its final form in Equation (19). The coefficients in Equation (20) are rewritten in the circular rigid foundation case as

$$\left.\begin{aligned} D_n &= aH_{n/\nu}^{(1)'}(ka)\int_0^{\nu\pi}\cos\left(\frac{n\theta}{\nu}\right)d\theta \\ d_n &= aJ_{n/\nu}^{'}(ka)\int_0^{\nu\pi}\cos\left(\frac{n\theta}{\nu}\right)d\theta \end{aligned}\right\} \tag{24}$$

It should be noted that the second term in Equations (20) vanish as the angle α, the angle between the normal and radial directions, is zero. The integrals in Equation (20) will vanish for all n not equal to 0, and have a value of $\nu\pi$ at $n = 0$. The equation represented by Equation (19) reduces to

$$aH_0^{(1)'}(ka).\nu\pi.A_0 + \left(\frac{\rho_f}{\rho}\right)k^2\left(\frac{\nu\pi a^2}{2}\right)\Delta = -aJ_0^{'}(ka).\nu\pi.\frac{2}{\nu} \tag{25}$$

where the area of the semi-circular rigid foundation is given by $\nu\pi a^2/2$, and $a_0 = 2/\nu$. By substituting $-k^*H_1^{(1)}(ka)$ for $H_0^{(1)'}(ka)$, and $-k^*J_1(ka)$ for $J_0'(ka)$, the above equation is now written as

$$-A_0H_1^{(1)}(ka) + \frac{ka}{2}\frac{\rho_f}{\rho}\Delta = \frac{2}{\nu}J_1(ka) \tag{26}$$

which is identical to the analytic solution (Dermendjian and Lee, 2001).

The solution, represented by Equations (10), (11), (12) and (13), may be repeated here with the change of $r = a$ rather than $r = a(\theta)$. The equations represented in Equations (13) can thus be rewritten as for $m > 0$,

$$\left.\begin{aligned} C_{mn} &= H_{n/\nu}^{(1)}(ka)\int_0^{\nu\pi}\cos\left(\frac{n\theta}{\nu}\right)\cos\left(\frac{m\theta}{\nu}\right)d\theta \\ c_{mn} &= J_{n/\nu}(ka)\int_0^{\nu\pi}\cos\left(\frac{n\theta}{\nu}\right)\cos\left(\frac{m\theta}{\nu}\right)d\theta \end{aligned}\right\} \tag{27}$$

Utilizing the orthogonality of the cosine functions, i.e. for $m = n$, but not equal to zero, and zero for m not equal to n, the set of equations

$$\int_0^{\nu\pi}\cos\left(\frac{m\theta}{\nu}\right)\cos\left(\frac{n\theta}{\nu}\right)d\theta = \frac{\nu\pi}{2} \tag{28}$$

represented by Equation (12) are now reduced to

$$H_{n/\nu}^{(1)}(ka).\frac{\nu\pi}{2}.A_n = -J_{n/\nu}(ka).\frac{\nu\pi}{2}.\left(\frac{4}{\nu}e^{\frac{-in\pi}{2\nu}}\cos\left(\frac{n\gamma}{\nu}\right)\right) \tag{29}$$

which reduces to

$$A_n = \frac{-\frac{4}{\nu}e^{-\frac{in\pi}{2\nu}}\cos\left(\frac{n\gamma}{\nu}\right)J_{n/\nu}(ka)}{H_{n/\nu}^{(1)}(ka)} \tag{30}$$

which is again identical to the analytic solution (Dermendjian and Lee, 2001).

The matrix presented in Equation (12) is thus diagonal except for the 2×2 upper left portion which is coupled, representing the relationships between A_0 and Δ. This solution thus mirrors that of the analytical solution presented in the above reference.

In other words, the appropriate choice of the weight functions results in the exact closed form solution for the case of the semi-circular rigid foundation.

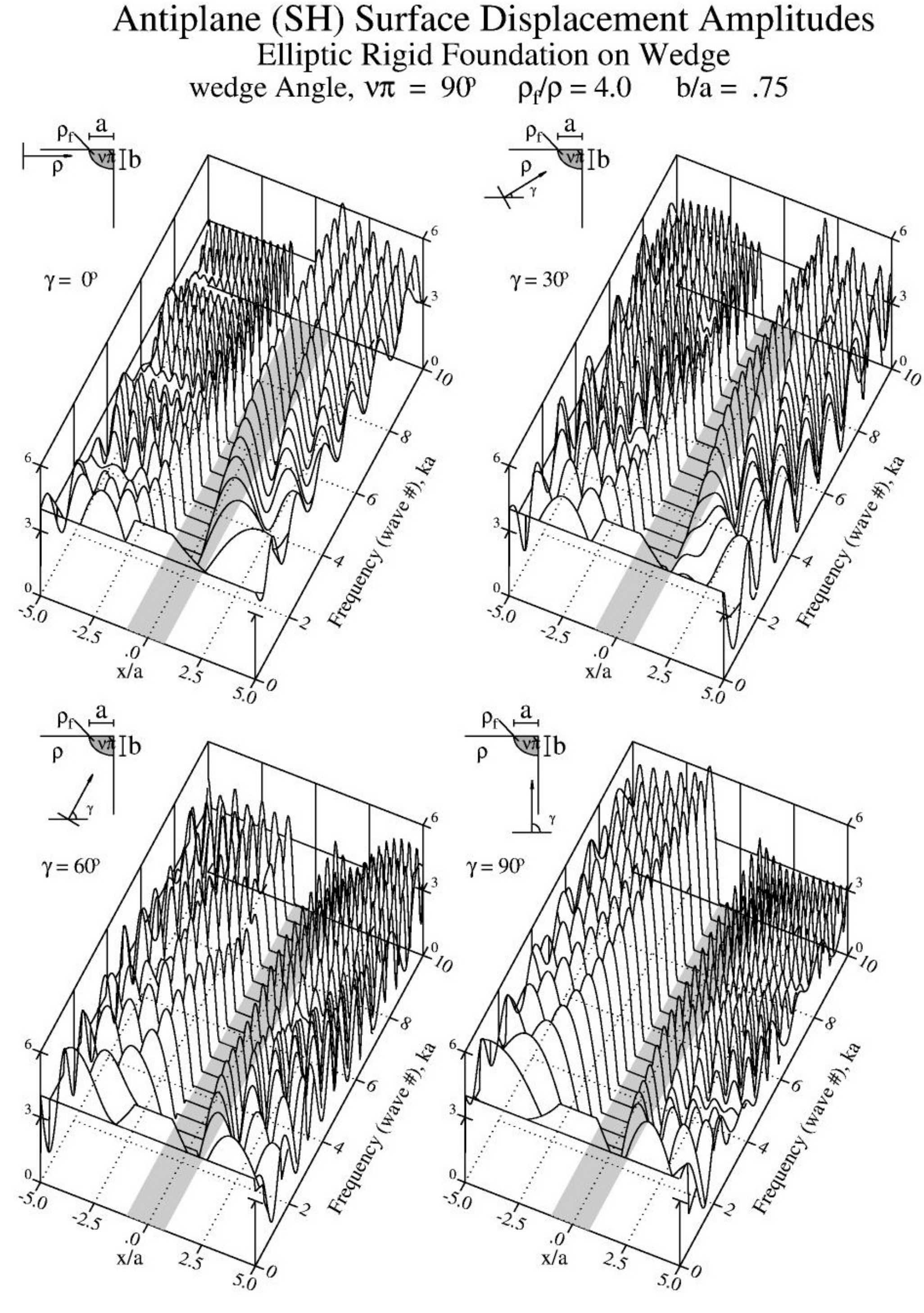

Fig. 2 Anti-plane surface displacement amplitudes: Elliptic rigid foundation

THE DISPLACEMENT AMPLITUDES

The above analyses for arbitrary-shaped rigid foundations are applied for the following cases of rigid foundations, where, in each case, the ratio of foundation density to soil density of $\rho_f/\rho = 4$ is used.

1. The Elliptic Rigid Foundation

The displacement amplitudes for elliptic rigid foundations are evaluated for the shape defined by

$$\left(\frac{x}{a}\right)^2 + \left(\frac{y}{b}\right)^2 = 1 \tag{31}$$

for ratios of *b/a* of 0.75 to 1.25. When the *b/a* ratio is 1, the shape is circular and is compared with the solution of Lee and Sherif (1996). The results of the circular rigid foundation on half space, where the wedge angle $\nu\pi$ = 180°, are compared with the existing analytic solutions presented by Trifunac (1973). The results of the elliptical rigid foundation on half space, where the wedge angle $\nu\pi$ = 180°, are compared with the existing analytic solutions presented by Dermendjian and Lee (2001).

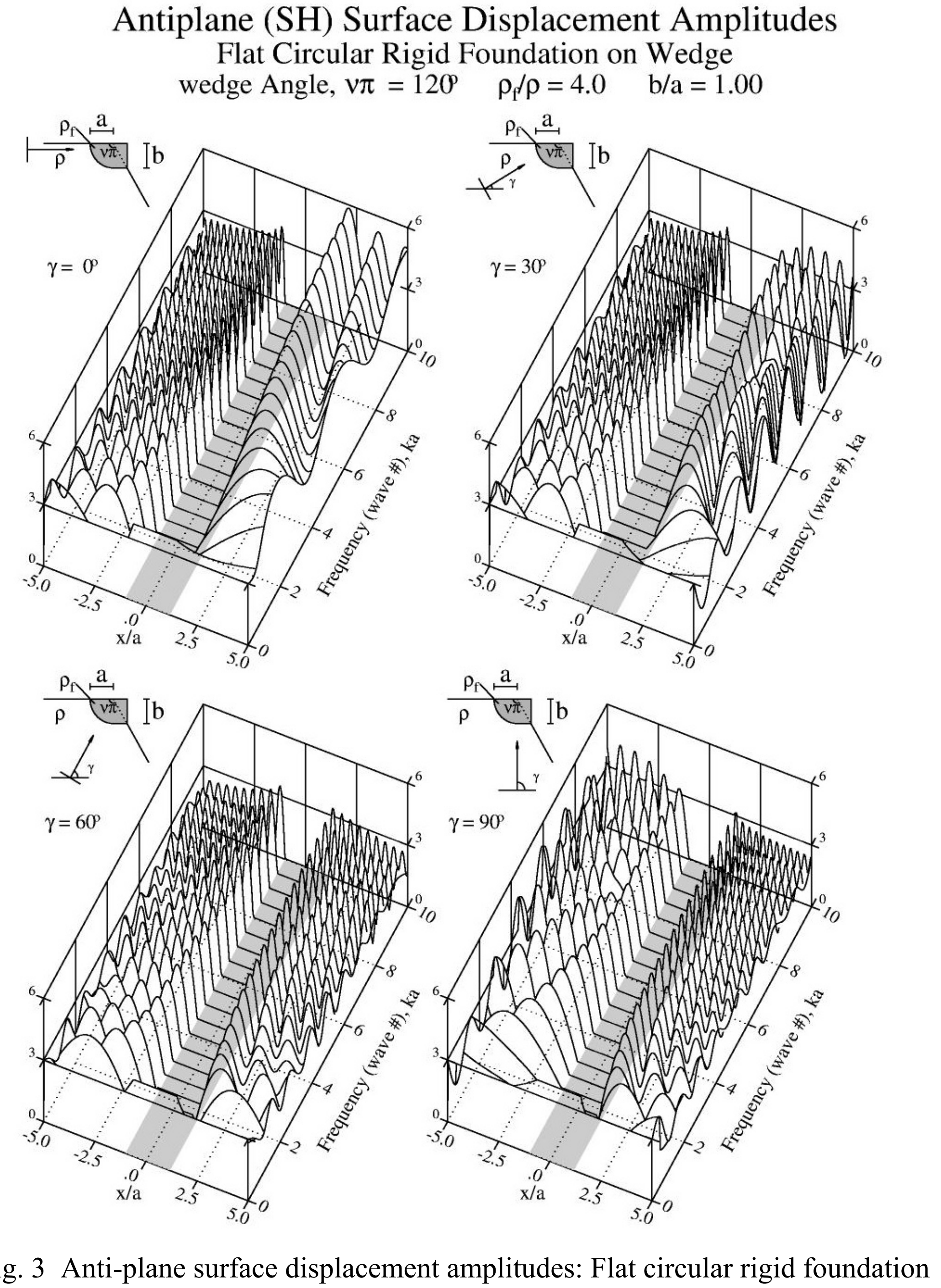

Fig. 3 Anti-plane surface displacement amplitudes: Flat circular rigid foundation

The wedge angles studied range from 90° to 180°, the cases of a quarter space to that of a flat half-space. Figure 2 is a representative graph representing the displacement amplitudes for elliptic rigid foundations with wedge angle of $\nu\pi$ = 90° and varying angles of incidence. The graphs are three-dimensional plots representing the displacement amplitudes for incident plane unit amplitude SH waves.

For all graphs, the displacement amplitudes are plotted versus the dimensionless distance *x/a* labeled to range between values of –5 and 5, and the frequency (wave number) *ka*, ranging between values of 0 and 10. Note that these distances are not the coordinates on the axis used, but are shown just for visual convenience. The labels *x/a* < –1 thus correspond to points on the horizontal surface of the wedge-shaped half space to the left of the rigid foundation. Distances –1 < *x/a* < *b/a* (the shaded part in the figure) correspond to points on the surface of the rigid foundation, and distances *x/a* > *b/a* correspond to points on the inclined surface of the wedge-shaped half space to the right of the rigid foundation. The origin is taken as shown in Figure 1, at the point of intersection of the horizontal and the inclined surfaces of the wedge with the positive *x*-axis to the left of the origin and the positive *y*-axis vertically downward.

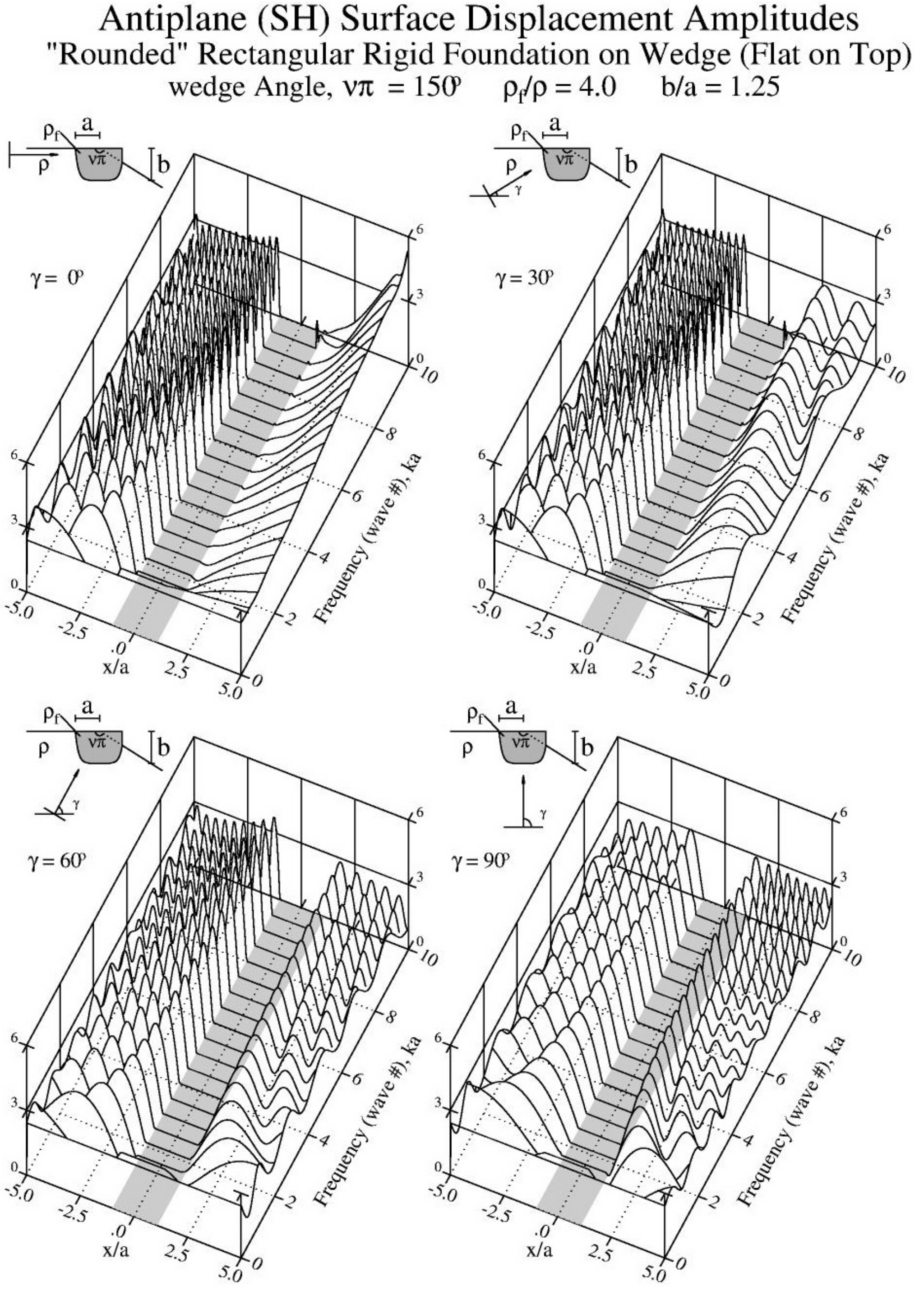

Fig. 4 Anti-plane surface displacement amplitudes: "Rounded" rectangular rigid foundation

In addition, for all graphs, the stress-free boundary condition on the horizontal and the inclined surfaces of the wedge-shaped half space, i.e. where *x/a* < –1 and *x/a* > *b/a,* are automatically satisfied and thus no integration is carried out at those surfaces. Integration is carried out on the points that are on the surface of the rigid foundation by using the (moment) method of weighted-residuals.

In the absence of the rigid foundation, the maximum free-field displacement amplitude in a quarter space is 4. In the presence of the rigid foundation, the maximum displacement amplitudes higher than 6 is observed, corresponding to an amplification of over 1.5.

2. The Elliptic-Flat beyond 90° Rigid Foundation

The displacement amplitudes of elliptic rigid foundations with flat surface beyond 90° are evaluated for the shape defined by Equation (9) earlier for the elliptic part of the rigid foundation and by a flat surface for the surface beyond 90°. The analyses can again be performed for various b/a ratios of 0.75 to 1.25. The wedge angles of interest are again from 90° to 180°. Figure 3 is a representative graph representing the displacement amplitudes for elliptic rigid foundations with flat surface beyond 90° with wedge angle of 120° and four angles of incidence.

In the absence of the rigid foundation, the maximum free-field displacement amplitude in a 120° ($\nu\pi = 2\pi/3$) wedge space is $2/\nu = 3$. In the presence of the rigid foundation, the maximum displacement amplitudes close to 6 (the case of horizontal incidence) are again observed, corresponding to an amplification close to 2.

3. The Rounded-Rectangular Rigid Foundation

The displacement amplitudes for rounded-rectangular rigid foundations are evaluated for the shape defined by

$$\frac{y}{a} = \frac{b}{a}\left[1 - e^{-\alpha\left(1-\frac{|x|}{a}\right)}\right] \tag{32}$$

where $\alpha > 0$ is a positive integer large enough so that the graph of the function resembles a rectangular shape with "rounded" corner. In this analysis, a value of $\alpha = 8$ is used. Again, the analyses and calculations can range for b/a ratios of 0.75 to 1.25, and for wedge angles from 90° to 180°. Figure 4 is a representative graph representing the displacement amplitudes for rounded-rectangular rigid foundations with wedge angle of $\nu\pi = 150°$ and four angles of incidence.

In the absence of the rigid foundation, the maximum free-field displacement amplitude in a 150° ($\nu\pi = 5\pi/6$) wedge space is $2/\nu = 2.4$. In the presence of the rigid foundation, the maximum displacement amplitudes close to 5 (the case of horizontal incidence) are again observed, corresponding to an amplification of over 2.

For the weighted-residual method, as many as $N = 20$ terms are used to achieve convergence at high frequencies. The agreement of the results with the existing analytic solutions is good.

CONCLUSIONS

The displacement amplitudes calculated on or near arbitrary-shaped wedge-shaped rigid foundations show that the response is dependent on all the parameters used in the analysis, including but not limited to the angle of incidence, frequency of the incoming train of the SH waves, the geometry of the rigid foundation and the material properties of the media. The reader is referred to Dermendjian (2002), and Dermendjian and Lee (2003) for a more complete set of case-studies.

In the absence of the rigid foundation, the maximum free-field displacement amplitude in a wedge-shaped half-space with wedge angle $\nu\pi$ is $2/\nu$. The wedge spaces studied in this paper range from the case of a quarter space to a flat half-space ($1/2 \le \nu \le 1$). In the presence of the rigid foundation, the maximum displacement amplitudes higher than 6 (the case of horizontal incidence) are observed, and they correspond to an amplification of over 2.

The present case of an arbitrary-shaped cylindrical rigid foundation on the vertex of a wedge space is an extension of the same problem in a flat half space, and the case of an arbitrary-shaped cylindrical canyon in a wedge space. While there are not much practical rigid foundation topographies that will fit the geometry of the rigid foundations studied here, the present paper presents the methodology from which it may be possible that more complicated problems are built on and solved. For example, the same weighted-residual moment method may next be applied to arbitrary-shaped foundations in Soil-Structure-Interaction (SSI) studies on wedge-shaped half-space.

REFERENCES

1. Achenbach, J.D. (1973). "Wave Propagation in Elastic Solids", North-Holland Publishing Company, U.S.A.
2. Cao, H. and Lee, V.W. (1989). "Scattering of Plane SH Waves by Circular Cylindrical Rigid Foundations of Various Depth-to-Width Ratios", European Earthquake Engineering, Vol. II, pp. 29-37.
3. Cao, H. and Lee, V.W. (1990). "Scattering and Diffraction of Plane P Waves by Circular Cylindrical Rigid Foundations with Variable Depth-to-Width Ratios", Soil Dynamics and Earthquake Engineering, Vol. 9, No. 3, pp. 141-150.
4. Chang, W.L. (1990). "Boundary Integral Equation Method for the Diffraction of Elastic Waves Using Simplified Green's Functions", Ph.D. Thesis, Univ. of Southern California, Los Angeles, California, U.S.A.
5. Croisille, J.-P. and Lebeau, Gilles (1999). "Diffraction by an Immersed Elastic Wedge", Lecture Notes in Mathematics, Series No. 1723, Springer-Verlag, Germany.
6. Dermendjian, N. (2002). "Soil-Structure Interaction and Diffraction of Anti-plane (SH) Waves around Topographies in a Wedge-Shaped Elastic Half-Space", Ph.D. Thesis, Univ. of Southern California, Los Angeles, California, U.S.A.
7. Dermendjian, N. and Lee, V.W. (2001). "Anti-plane Deformations near an Arbitrary-Shaped Rigid Foundation in a Wedge-Shaped Elastic Half-Space", Proceedings of 15th ASCE Engineering Mechanics Conference, Univ. of California, San Diego, U.S.A., p. 1.
8. Dermendjian, N. and Lee, V.W. (2003). "Anti-plane Soil-Structure Interaction on a Circular Rigid Foundation in an Elastic Wedge-Shape Half-Space", ASME Mechanics and Materials Conference, Camelback Inn Resort, Scottsdale, Arizona, U.S.A., June 17-20.
9. Graff, K.F. (1991). "Wave Motion in Elastic Solids", Ohio State University Press, U.S.A.
10. Harrington, R.F. (1967). "Matrix Methods for Field Problems", Proceedings of IEEE, Vol. 55, No. 2.
11. Lee, V.W. (1982). "A Note on the Scattering of Elastic Plane Waves by a Hemispherical Rigid Foundation", International Journal of Soil Dynamics and Earthquake Engineering, Vol. 1, No. 3, pp. 122-129.
12. Lee, V.W. (1984). "Three-Dimensional Diffraction of Plane P, SV and SH Waves by a Hemispherical Alluvial Valley", International Journal of Soil Dynamics and Earthquake Engineering, Vol. 3, No. 3, pp. 133-144.
13. Lee, V.W. (1988). "Three-Dimensional Diffraction of Elastic Waves by a Spherical Cavity in an Elastic Half-Space, I: Closed-Form Solutions", International Journal of Soil Dynamics and Earthquake Engineering, Vol. 7, No. 3, pp. 149-167.
14. Lee, V.W. (1990). "On the Scattering of Plane SH Waves by a Semi-parabolic Cylindrical Cavity in an Elastic Half-Space", Geophysical Journal, Vol. 100, pp. 79-86.
15. Lee, V.W. and Cao, H. (1989). "Diffraction of SV Waves by Circular Cylindrical Rigid Foundations of Various Depths", Journal of Engineering Mechanics, ASCE, Vol. 115, No. 9, pp. 2035-2056.
16. Lee, V.W. and Manoogian, M.E. (1995). "Surface Motion above an Arbitrary Shaped Underground Cavity for Incident SH Waves", European Earthquake Engineering, Vol. VIII, No. 1, pp. 3-11.
17. Lee, V.W. and Sherif, R. (1996). "Diffraction around Circular Rigid Foundation in Elastic Wedge Space by Plane SH-Waves", Journal of Engineering Mechanics, ASCE, Vol. 122, No. 6, pp. 539-544.
18. Lee, V.W. and Wu, X. (1994a). "Application of the Weighted Residual Method to Diffraction by 2-D Rigid Foundations of Arbitrary Shape: I. Incident SH Waves", Soil Dynamics and Earthquake Engineering, Vol. 13, No. 5, pp. 355-364.

19. Lee, V.W. and Wu, X. (1994b). “Application of the Weighted Residual Method to Diffraction by 2-D Rigid Foundations of Arbitrary Shape: Incident P, SV and Rayleigh Waves”, Soil Dynamics and Earthquake Engineering, Vol. 13, No. 5, pp. 365-373.
20. Luco, J.E., Wong, H.L. and Trifunac, M.D. (1975). “A Note on the Dynamic Response of Rigid Embedded Foundations”, Earthquake Engineering and Structural Dynamics, Vol. 4, No. 2, pp. 119-127.
21. Marzeda, J., Pauk, V. and Woz'niak, M. (2003). “Biparametric Models for Elastic Wedge Foundation”, Journal of Engineering Mechanics, ASCE, Vol. 129, No. 1, pp. 88-93.
22. Mow, C.C. and Pao, Y.H. (1971). “The Diffraction of Elastic Waves and Dynamic Stress Concentrations”, Report R-482-PR, RAND Corporation, Santa Monica, U.S.A.
23. Pozharki, D.A. (2000). “Three-Dimensional Contact Problem for an Elastic Wedge with Allowance for Friction in an Unknown Contact Region”, Doklady Physics, Vol. 45, No. 5, pp. 236-240.
24. Sanchez-Sesma, F.J. (1985). “Diffraction of Elastic SH-Waves in Wedges”, Bulletin of the Seismological Society of America, Vol. 75, No. 5, pp. 1435-1446.
25. Sanchez-Sesma, F.J. and Rosenbleuth, E. (1979). “Ground Motion at Rigid Foundations of Arbitrary Shape under Incident SH-Waves”, Earthquake Engineering and Structural Dynamics, Vol. 7, pp. 441-450.
26. Trifunac, M.D. (1973). “Scattering of Plane SH Waves by a Semi-Cylindrical Rigid Foundation”, Earthquake Engineering and Structural Dynamics, Vol. 1, pp. 267-281.
27. Wong, H.L. and Trifunac, M.D. (1974a). “Scattering of Plane SH Waves by Semi-Elliptical Rigid Foundations”, Earthquake Engineering and Structural Dynamics, Vol. 3, pp. 157-169.
28. Wong, H.L. and Trifunac, M.D. (1974b). “Surface Motion of a Semi-Elliptical Alluvial Valley for Incident Plane Waves”, Bulletin of the Seismological Society of America, Vol. 64, pp. 1389-1408.
29. Wong, H.L., Trifunac, M.D. and Westermo, B. (1977). “Effects of Surface and Subsurface Irregularities on the Amplification of Monochromatic Waves”, Bulletin of the Seismological Society of America, Vol. 67, pp. 353-368.